Development of a rotary pneumatic transformer

Stephan Merkelbach*, Olivier Reinertz and Hubertus Murrenhoff*

RWTH Aachen University, Institute for Fluid Power Drives and Systems (IFAS),
Campus-Boulevard 30, D-52074 Aachen, Germany*
E-Mail: stephan.merkelbach@ifas.rwth-aachen.de

Pneumatic drives are widely used in industrial applications. As the energy demand of production systems becomes more and more important, nowadays, many users favour a reduction of the general supply pressure to save energy. Nevertheless, some applications afford compact and powerful drives. To serve these demands, an energy efficient local pressure boosting is necessary. Today, linear pressure boosters based on double-piston cylinders are used to fulfil this task. The paper proposes a novel concept based on pneumatic radial piston motors. The new concept features a radial piston compressor, which is driven by a radial piston motor. The paper shows simulation data as well as a validation by experimental investigations of a working model of the new booster. Different configurations of the booster are examined for a range of driving pressures and pressure ratios. The experimental results are compared to a standard pneumatic booster subsequently.

Keywords: Pneumatics, Energy Efficiency, Pressure Booster
Target audience: Pneumatics, Automation

1 Introduction

Pneumatic drives are used in a great variety of applications, especially in manufacturing and process engineering. Since compressed air is an expensive form of energy, recent developments show a tendency to lower the overall system pressure in compressed air systems. This improvement should lead to lower energy consumption in the compressor while larger drives are needed to provide equivalent driving forces /1/. Despite that, some applications require compact drives and, therefore, a higher driving pressure. To ensure the applicability of these drives while maintaining the energy efficiency it is suitable to implement pressure boosters.

Current concepts for pressure boosters feature double piston linear transformers which have a very limited efficiency. To enhance the efficiency of pneumatic transformers, the paper proposes a novel concept featuring rotating units. The new transformer comprises of a pneumatic radial piston motor which drives a radial piston compressor. Similar concepts using pumps and motors are well known by hydraulic systems /1–3/. These hydraulic transformers are used, e.g., for energy recovery in mobile or stationary systems. Hydraulic transformers are often built using axial piston machines. In these units, the separation between high and low pressure and the valve function are realised using a valve plate. Due to the low viscosity of air, control using a valve plate is not possible as the leakage through the gaps would cause very high losses which negatively impact the efficiency of the booster. Therefore, an actuation using switching and check valves is proposed.

1.1 Standard Booster

Standard pneumatic boosters that are used in industrial applications today are designed as double piston cylinders, as shown in figure 1. The double piston fulfils an alternating stroke from one side to the other. In each cycle, one of the inner chambers is used for the compression of the output air. One driving chamber and the other inner chamber work as driving chambers for the compression. The second driving chamber is exhausted to the environment. The ratio between input and output mass flow as well as between input and output pressure is defined by the ratio between the piston areas used for driving and compression, respectively. The switching valve is actuated pneumatically which is not shown in the figure for readability.

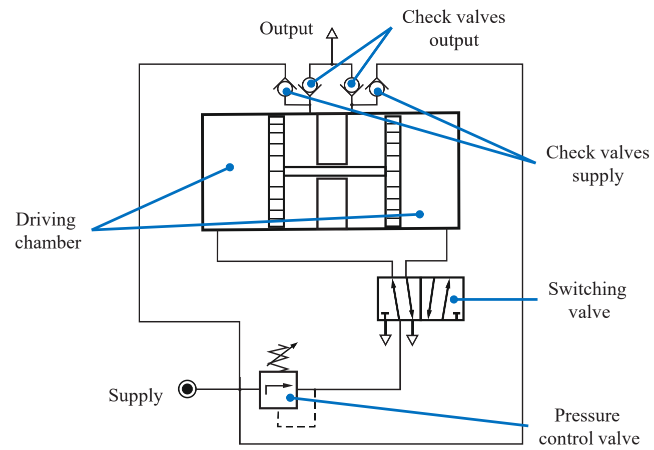

Figure 1: Working principle of a standard pneumatic booster

Most boosters offer the possibility to reduce the driving pressure in the driving chambers. Due to the force equilibrium at the piston the output pressure is decreased. As the air in the outer driving chambers is exhausted to the environment at the end of each cycle, a lower driving pressure in these chambers also increases the efficiency of the booster because less air is filled into the chamber. Standard double piston boosters emit a lot of noise due to the nearly undamped end stops of the piston. The efficiency of an exemplary piston booster is examined in chapter 4 of the paper.

2 Novel booster concept

Figure 2 shows a schematic of the novel design. The booster consists of a pneumatic radial piston motor shown on the left hand side and a radial piston compressor shown on the right.

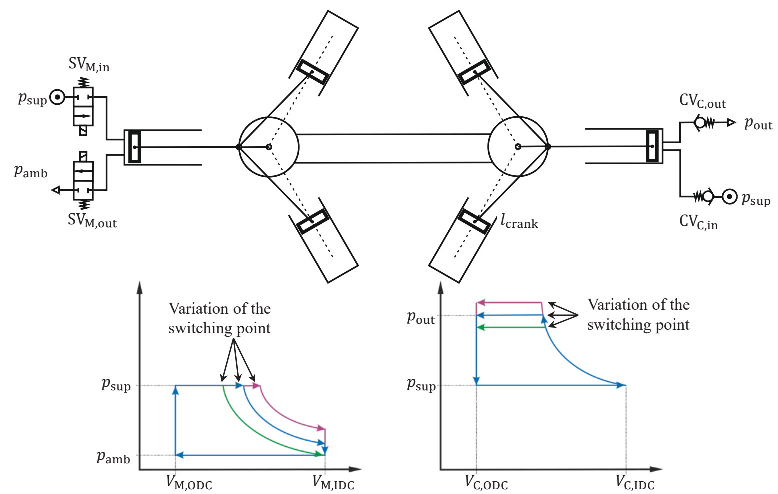

Figure 2: Working principle and p-V-diagram of the novel pressure booster concept

The transformer takes in air at supply pressure p_{sup} in order to compress it to a higher outlet pressure p_{out}. The energy needed for the compression process is supplied by the pneumatic motor shown on the left side. Each piston is actuated by two switching valves. The compressor (right hand side) is controlled by two check valves per cylinder connecting the chamber to the supply and outlet, respectively. For clarity reasons, the valves are depicted for one cylinder of both motor and compressor only.

Additionally, the p-V-diagrams of the motor and compressor are shown in figure 2. Due to the actuation of the motor by means of switching valves, an adjustment of the motor characteristics is possible. A variation of the piston's radial position at which the connection to the air supply is cut off influences the air mass fed to the motor. Earlier switching off does not only lead to lower air consumption and therewith higher efficiency but also reduces the mean driving torque of the motor and therewith the maximum output pressure of the compressor which is directly proportional to the mean torque.

3 Simulation model

To establish the main influences on the efficiency of the novel pneumatic booster, a lumped parameter simulation model was developed. The following pages present the mathematical description of the booster, its implementation in the simulation environment and some sample results of the simulation study.

3.1 Mathematical description

To understand the working principle and the main influences on the exergy efficiency of the booster, a mathematical description of the kinematics, thermodynamics and the effect of the dead volume attached to each cylinder is of great importance. This description is shown in paragraphs 3.1.1 to 3.1.3.

3.1.1 Kinematic model

Figure 2 shows a schematic of one cylinder including the crank drive which converts the linear movement of the piston into a rotational movement of the shaft. The conversion from rotational movement to linear movement is mainly dependent on the push rod ratio $\lambda_{\mathrm{s}} = \frac{l_{\mathrm{crank}}}{l_{\mathrm{rod}}}$. /4/

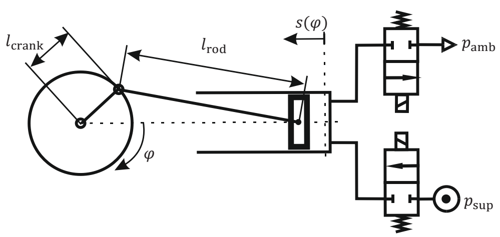

Figure 3: Geometry of one motor piston including valves, crank and rod

For $\lambda_{\mathrm{s}}^2 \ll 1$ the piston stroke and velocity can be calculated using (1) and (2) respectively. As the rod ratio of the radial piston motors examined in this study lies between 0.125 and 0.156, this assumption is valid.

$$s(\varphi) = l_{\mathrm{crank}} \cdot \left[1 - \cos(\varphi) + \frac{1}{4} \cdot \lambda_{\mathrm{s}} \cdot (1 - \cos(2\varphi))\right] \tag{1}$$

$$\dot{s}(\varphi) = \frac{ds(\varphi)}{dt} = \frac{ds(\varphi)}{d\varphi}\omega = l_{\mathrm{crank}} \cdot \dot{\varphi} \cdot \sin(\varphi) + \frac{1}{2} \cdot \lambda_{\mathrm{s}} \cdot \sin(2\varphi) \tag{2}$$

The torque M_{press} produced by the pressure force $F_{\mathrm{G}} = \Delta p \cdot A_{\mathrm{piston}}$ can then be calculated using equation (3) with $\gamma = \arcsin\left(\frac{l_{\mathrm{crank}}}{l_{\mathrm{rod}}} \cdot \sin\varphi\right)$.

$$M_{\mathrm{press}} = F_{\mathrm{TG}} \cdot l_{\mathrm{crank}} = \frac{\cos(90° - \varphi - \gamma)}{\cos\gamma} \cdot F_{\mathrm{G}} \cdot l_{\mathrm{crank}} \tag{3}$$

The rotational acceleration $\ddot{\varphi}$ is then calculated from the conservation of angular momentum using equation (4) with the sum of driving torque produced by the motor, load torque applied by the compressor and the torque losses M_{loss} caused by friction.

$$J_{\mathrm{tot}} \cdot \ddot{\varphi} = \sum_{i=1}^{n=n_{\mathrm{p,M}}} M_{\mathrm{press},i} - \sum_{j=1}^{n=n_{\mathrm{p,C}}} M_{\mathrm{press},j} - M_{\mathrm{loss}} \tag{4}$$

3.1.2 Thermodynamic modeling

Equation (5) delivers the calculation of the pressure change in each cylinder chamber. The total pressure change is calculated as the sum of the pressure change due to mass transfer into and out of the chamber $\dot{p}_{\dot{m}}$, the pressure change $\dot{p}_{HE}$ caused by heat exchange between air and cylinder walls and the pressure change $\dot{p}_{\dot{V}}$ due to the volume change of the cylinder chamber in the cause of the rotational movement. /5/

$$\dot{p} = \dot{p}_{\dot{m}} + \dot{p}_{HE} + \dot{p}_{\dot{V}} \tag{5}$$

To examine the efficiency of the booster, the thermodynamic concept of exergy is used. Exergy describes the ability to conduct work of different forms of energy. The exergy fed to a pneumatic system can be calculated using equation (6). This includes the compressed air mass flow as well as the electrical energy fed e.g. to the valves. /6/

$$\begin{aligned} \Delta E_{\mathrm{in}} &= \Delta m_{\mathrm{air}} \cdot [(h_{\mathrm{air}} - h_{\mathrm{amb}}) - T_{\mathrm{amb}}(s_{\mathrm{air}} - s_{\mathrm{amb}})] + W_{\mathrm{el,in}} \\ &= \Delta m_{\mathrm{air}} \cdot \left[c_{\mathrm{p,air}} \cdot (T_{\mathrm{air}} - T_{\mathrm{amb}}) - T_{\mathrm{air}}\left(c_{\mathrm{p,air}} \ln\left(\frac{T_{\mathrm{air}}}{T_{\mathrm{amb}}}\right) - \mathrm{R}\ln\left(\frac{p_{\mathrm{air}}}{p_{\mathrm{amb}}}\right)\right)\right] + W_{\mathrm{el,in}} \end{aligned} \tag{6}$$

As described in /7/, an analysis using exergy instead of energy is advantageous for pneumatic systems because the influence of different losses on the overall efficiency can be quantified more easily. Additionally, effects that have a small influence on the working ability of a system can be neglected during an optimisation of automation systems.

The exergy efficiency is then defined according to equation (7) as the ratio between the output exergy ΔE_{out} and the input exergy ΔE_{in} over a certain period of time. The total energy consumed by the valves is around 6000 J for one cycle shown in chapter 4. Due to its small amount in relation to the exergy contained in the compressed air mass flow the electrical energy $W_{\mathrm{el,in}}$ is neglected in the following.

$$\zeta = \frac{\Delta E_{\mathrm{out}}}{\Delta E_{\mathrm{in}}} = \frac{\Delta m_{\mathrm{air,out}} \cdot \left[\left(h_{\mathrm{air,out}} - h_{\mathrm{amb}}\right) - T_{\mathrm{amb}}\left(s_{\mathrm{air,out}} - s_{\mathrm{amb}}\right)\right]}{\Delta m_{\mathrm{air,in}} \cdot \left[\left(h_{\mathrm{air,in}} - h_{\mathrm{amb}}\right) - T_{\mathrm{amb}}\left(s_{\mathrm{air,in}} - s_{\mathrm{amb}}\right)\right]} \tag{7}$$

If an isothermal change of state is assumed, equation (7) can be simplified to equation (8). This assumption is valid for the described booster if cooling the air to ambient temperature in the accumulator is taken into account.

$$\zeta = \frac{\Delta E_{\mathrm{out}}}{\Delta E_{\mathrm{in}}} = \frac{\Delta m_{\mathrm{air,out}} \cdot \ln\left(\frac{p_{\mathrm{out}}}{p_{\mathrm{amb}}}\right)}{\Delta m_{\mathrm{air,in}} \cdot \ln\left(\frac{p_{\mathrm{in}}}{p_{\mathrm{amb}}}\right)} \tag{8}$$

In the study, the exergy efficiency is calculated according to the definition presented in equation (8).

3.1.3 Influence of the dead volume

The dead volumes of compressor and motor have major influence on the maximum efficiency which can be obtained by the booster. Therefore, a mathematical model of this influence is presented as follows.

Without consideration of leakage, the mass flow $\dot{m}_{\mathrm{sup}}$ fed to the booster can be calculated as the sum of the theoretical input mass flows into motor and compressor according to equation (9).

$$\dot{m}_{\mathrm{sup}} = \dot{m}_{\mathrm{in,theo,M}} + \dot{m}_{\mathrm{in,theo,C}} \tag{9}$$

As the motor cylinder chambers are completely exhausted at the end of each rotational cycle, the theoretical input mass flow (without leakage losses) to the motor can be calculated by the chamber pressure at the inner dead center (IDC).

$$\dot{m}_{\mathrm{in,theo,M}} = z_{\mathrm{cyl,M}} \cdot \left(V_{\mathrm{cyl,M}} + V_{\mathrm{dead,M}}\right) \cdot \rho_{\mathrm{IDC,M}} \cdot z_{\mathrm{cyl,M}} \cdot n \tag{10}$$

To calculate the theoretical output mass flow, the density at output pressure is needed. $V_{\mathrm{comp,C}}$ describes the part of the chamber volume which needs to be compressed to reach the output pressure. The dead volume $V_{\mathrm{dead,C}}$ influences the size of $V_{\mathrm{comp,C}}$ and therewith the efficiency of the booster. It is only filled with compressed air once, since it is not exhausted to the environment.

$$\dot{m}_{\mathrm{out,theo,C}} = z_{\mathrm{cyl,C}} \cdot \left(V_{\mathrm{cyl,C}} - V_{\mathrm{comp,C}}\right) \cdot \rho_{\mathrm{out}} \cdot z_{\mathrm{cyl,C}} \cdot n \tag{11}$$

Equation (12) describes the calculation of the volume $V_{p,\mathrm{out}}$ at which the output pressure is reached. Transforming this equation delivers equation (13) for the compression volume $V_{\mathrm{comp,C}}$.

$$\frac{p_{\mathrm{sup}}}{p_{\mathrm{out}}} = \left(\frac{V_{p,\mathrm{out}}}{V_{\mathrm{cyl,C}} + V_{\mathrm{dead,C}}}\right)^{n} = \left(\frac{V_{\mathrm{cyl,C}} + V_{\mathrm{dead,C}} - V_{\mathrm{comp,C}}}{V_{\mathrm{cyl,C}} + V_{\mathrm{dead,C}}}\right)^{n} \tag{12}$$

$$\Rightarrow V_{\mathrm{comp,C}} = \left(V_{\mathrm{cyl,C}} + V_{\mathrm{dead,C}}\right) \cdot \left(1 - \left(\frac{p_{\mathrm{sup}}}{p_{\mathrm{out}}}\right)^{\frac{1}{n}}\right) \tag{13}$$

Inserting equation (13) in equation (11) leads to equation (14) for the theoretical output mass flow of the compressor in dependence of the inverted pressure ratio $\frac{p_{\mathrm{sup}}}{p_{\mathrm{out}}}$.

$$\dot{m}_{\mathrm{out,theo,C}} = \left(V_{\mathrm{cyl,C}} \cdot \left(\frac{p_{\mathrm{sup}}}{p_{\mathrm{out}}}\right)^{\frac{1}{n}} + V_{\mathrm{dead,C}} \cdot \left(\left(\frac{p_{\mathrm{sup}}}{p_{\mathrm{out}}}\right)^{\frac{1}{n}} - 1\right)\right) \cdot \rho_{\mathrm{out}} \cdot z_{\mathrm{cyl,C}} \cdot n \tag{14}$$

Figure 4 shows the influence of the compressor dead volume on the output mass flow for both isothermal ($n = 1$) and isentropic ($n = 1.4$) compression. The dead volume has been normalised to the cylinder volume whereas the output mass flow was normalised to the value which is reached with no dead volume for each pressure ratio.

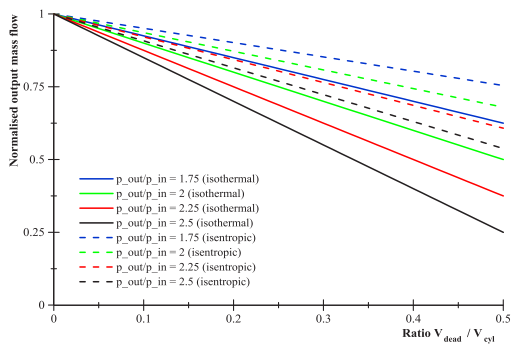

Figure 4: Influence of the dead volume on the output mass flow of the compressor

It is obvious, that even a relatively small dead volume of only 10 % of the chamber volume reduces the output mass flow and, therewith, the efficiency of the booster by more than 10 % for an isothermal compression with a pressure ratio of 2.5. In the functional model presented in chapter 4, off-the-shelf-components were used. This leads to a relatively large percentage of dead volume in comparison to the cylinder chamber volume. In case of the small compressor with 22 mm piston diameter, the dead volume is nearly one quarter of the chamber volume. In this case, the maximum output mass flow is reduced by up to one third.

3.2 Implementation

An excerpt of the simulation model implemented in DSHplus is shown in Figure 5. Both the motor and the compressor are modelled using a combination of a pneumatic cylinder and a thrust crank.

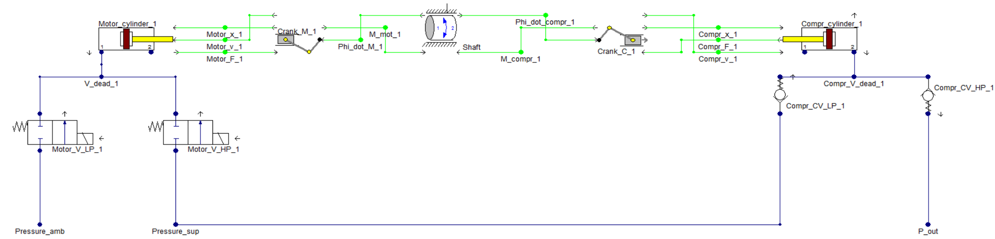

Figure 5: Excerpt of the simulation model in DSHplus

The torque delivered by the thrust cranks works as an input to a common shaft which comprises the inertia of the booster. Additionally, velocity dependent friction is calculated in the model of the rotating mass. The rotational position and velocity are then fed back to the thrust cranks where they are converted to the radial position and velocity of the cylinders where the piston force and the chamber pressure are calculated. The specific cylinder model used in the simulations does not include friction losses.

3.3 Simulation results

In the following, some sample results with high influence on the design of rotary pneumatic boosters are shown. Results towards exergy efficiency are presented for different configurations that were analysed in the study.

3.3.1 Exergy efficiency

Different configurations of motor and compressor geometry were included in the research. In all variations a five cylinder motor was implemented in combination with a three or five cylinder compressor. For both motor and compressor, the piston diameter, the crank and rod length were varied on the basis of off-the-shelf pneumatic radial piston motors. The piston diameter values considered here are 22 mm, 32 mm and 44 mm respectively.

Table 1 gives an overview over some simulation results for the exergy efficiency for a configuration comprising of a five cylinder motor in combination with a three cylinder compressor with 32 mm piston diameter each.

Table 1: Exergy efficiency in dependence on the supply and output pressure (five cylinder motor, three cylinder compressor, 32 mm piston diameter)

	p_{out}			
p_{Sup}	**7 bar**	**8 bar**	**9 bar**	**10 bar**
4 bar	51,5 %	-	-	-
5 bar	56,8 %	40,4 %	36,6 %	-
6 bar	71,1 %	65,0 %	52,8 %	39,8 %

The results show a maximum efficiency of over 70 %. In this case, only a small pressure ratio of 7/6 was reached. For higher pressure ratio values, the efficiency is lower, yet an efficiency of more than 50 % is possible.

Variation of the piston diameter shows an increase in efficiency for larger pistons due to the lower impact of friction in comparison to the driving torque and especially to the lower losses caused by the dead volume. As the dead volume stays constant for all variations, its percentage of the cylinder chamber volume is lower and, therefore, a higher output mass flow can be realised.

4 Functional model

To validate the simulation results and to show the potential of the new transformer, a functional model was built. The experimental setup, the functional model itself and some experimental results are shown in the following.

4.1 Experimental setup

Figure 6 shows a schematic of the test rig used to investigate the pneumatic booster. The high pressure air is delivered into an accumulator with a volume of 5 l. To simulate pneumatic consumers, a valve downstream the accumulator is connected to the environment. Therewith, air is released and the pressure inside the accumulator decreases.

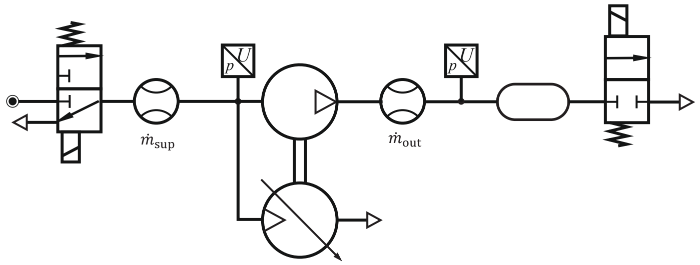

Figure 6: Schematic of the test rig

The test rig includes two mass flow sensors measuring the supply mass flow and the high pressure output mass flow, respectively. Additionally, the pressures upstream and downstream the booster are measured.

The working model developed in the study is shown in figure 7. It consists of a 5 cylinder radial piston motor (left) and a 3 piston radial piston compressor (right). To apply the standard radial piston motors, the cylinders were modified. New cylinders were designed to ensure sealing of the chambers and check as well as switching valves were implemented. The torque sensor between motor and compressor is used to define the rotational position of the shaft and, therewith, the radial positions of the pistons.

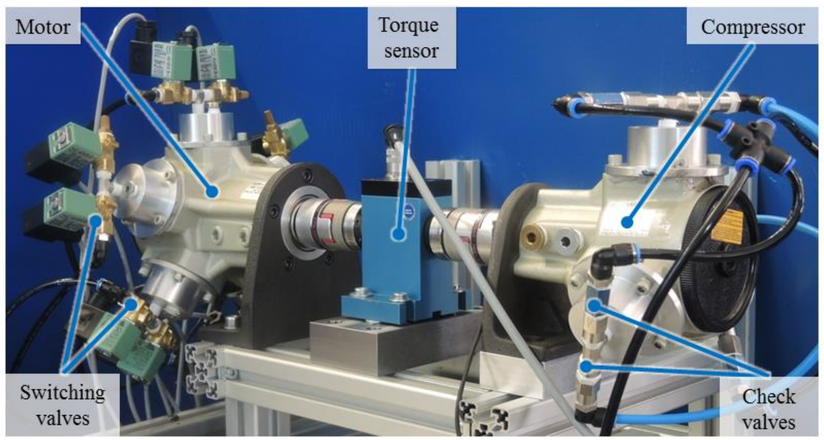

Figure 7: Pneumatic transformer of novel design concept (5 cylinder motor, three cylinder compressor)

In addition to the working model shown in figure 7, a second version comprising of a three piston compressor with a smaller piston diameter and a larger three piston motor was constructed and examined in the study. This smaller configuration is suitable for applications with lower demand for high pressure air but is still able to produce air at the same pressure ratio as the initial configuration.

4.2 Experimental results

4.2.1 Standard piston booster

Figure 8 shows sample experimental results for the exergy efficiency of a standard pneumatic booster in double piston configuration. The set up used for the investigation equals the set up for the novel booster concept. The absolute supply pressure was set to 5 bar. When the pressure inside the accumulator reaches 7.5 bar, the booster is switched off and the volume is exhausted to the environment. At a pressure lower than 7 bar, the booster restarts.

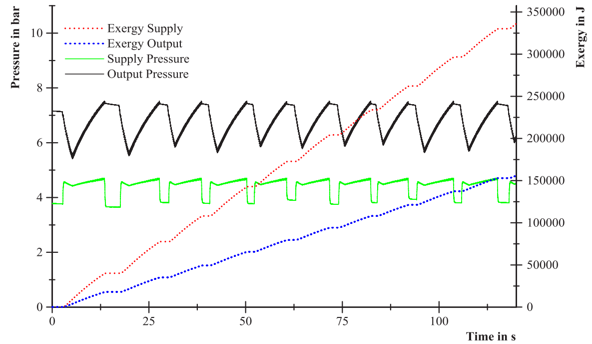

Figure 8: Experimental results for exergy and pressure for a standard pressure booster

The input and output exergy shown in figure 8 leads to an exergy efficiency of 47 %. An overview over the exergy efficiency obtained with the standard booster for different input pressure values as well as pressure ratios is given in table 2.

Table 2: Resulting exergy efficiency for different supply pressures and pressure ratios (standard double piston booster)

Supply pressure	Output pressure	Pressure ratio	Exergy efficiency
3.5 bar_{abs}	5-5.5 bar_{abs}	1.43-1.57	49.0 %
4 bar_{abs}	6-6.5 bar_{abs}	1.5-1.625	47.6 %
5 bar_{abs}	7-7.5 bar_{abs}	1.4-1.5	46.6 %
5 bar_{abs}	7.5-8 bar_{abs}	1.5-1.6	47.1 %

All values for the effiency lie within the range of 46 and 49 %.

4.2.2 Novel booster concept

First experimental results for a compression from a supply pressure of 5 bar_{abs} to an output pressure of 7 to 7.5 bar_{abs} are shown in figure 9. Besides the pressure in the supply line and inside the high pressure accumulator, the exergy fed to the booster and the output exergy are shown.

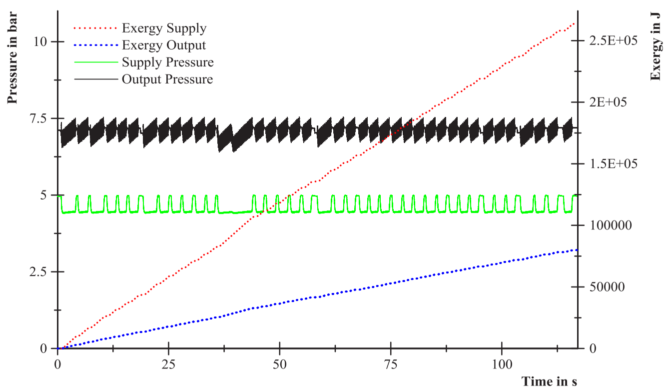

Figure 9: Experimental results for exergy and pressure without optimisation of the valve switching points (Five cylinder motor, three cylinder compressor)

To obtain these results, no optimisations of the actuation where put into action as the focus lies on the general functionality of the working model. The air supply is switched off at a rotational position of 150 °. This leads to a high driving torque and good dynamics of the booster. On the downside, the booster features a relatively poor exergy efficiency of 30 %. To increase this efficiency, an optimisation of the switching position was executed. The principle and results of this optimisation are described in depth in the following section.

4.2.3 Optimisation of switching positions

The variation of the switching points is depicted in figure 10. Without any optimisation, the air supply is switched off at a radial position of the piston which is near to the IDC. This leads to a very high mean torque of the motor but no expansion energy comprised in the air is used. Now, the switching point is moved closer to the outer dead center (ODC). This leads to a much smaller amount of air fed to the cylinder chamber and, therewith, a higher efficiency of the booster. On the downside, the maximum torque of the motor is reduced and the maximum pressure ratio decreases as well.

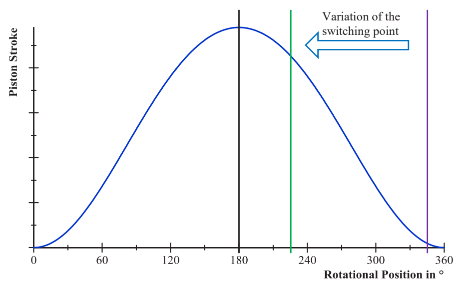

Figure 10: Variation of the switching point to reduce the input mass flow

The resulting values for the exergy supplied to the transformer and the exergy output to the accumulator are shown in figure 11. It is obvious, that the exergy supplied to the booster is much lower than before optimisation due to the lower mass flow into the booster. This leads to an exergy efficiency of 49.6 % which is increased significantly with respect to the initial approach shown in figure 9.

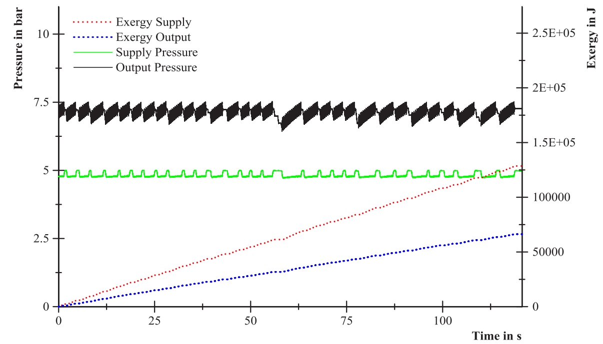

Figure 11: Experimental results for exergy and pressure after optimisation of the valve switching points (Five cylinder motor, three cylinder compressor)

Depending on the geometry of both motor and compressor and on the pressure ratio needed in the application, an optimisation of the switching point needs to be undertaken. In the study, the experimental investigation of the exergy efficiency was carried out at 4 different supply pressure values and pressure ratios. An overview over the results is given in table 3.

Table 3: Resulting exergy efficiency for different supply pressure and pressure ratio values (Five cylinder motor, three cylinder compressor)

Supply pressure	Output pressure	Pressure ratio	Min. angle at switching off	Exergy efficiency
3.5 bar_{abs}	5-5.5 bar_{abs}	1.43-1.57	240°	44.6 %
4 bar_{abs}	6-6.5 bar_{abs}	1.5-1.625	240°	45.3 %
5 bar_{abs}	7-7.5 bar_{abs}	1.4-1.5	225°	49.6 %
5 bar_{abs}	7.5-8 bar_{abs}	1.5-1.6	240°	59.5 %

The results show that the exergy efficiency of the novel booster lies in the range of 40-60 %. An increase of the supply pressure leads to an efficiency increase. At a constant supply pressure, a higher pressure ratio also improves the efficiency. These values are in the range of the values obtained using the standard booster. At a supply pressure of 5 bar_{abs} and an output pressure between 7.5 and 8 bar_{abs} the efficiency is better.

A smaller configuration, comprising of two three cylinder units with 32 mm piston diameter for the motor and 22 mm piston diameter for the compressor is also investigated. Exemplary results are shown in figure 12. In this case, the air supply was switched of at an angle of 60° after the ODC of the piston movement.

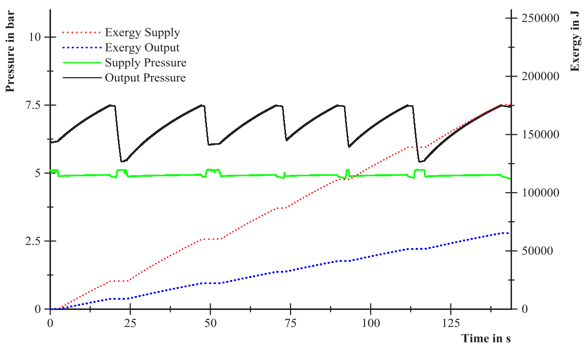

Figure 12: Experimental results for exergy and pressure after optimisation of the valve switching points (Three cylinder motor, small three cylinder compressor)

The results show a slower increase of the pressure inside the accumulator due to the smaller compressor. The exergy efficiency obtained here is 37.1 %. An overview over the experimental results is given in table 4.

Table 4: Resulting exergy efficiency for different supply pressure and pressure ratio values (Three cylinder motor, small three cylinder compressor)

Supply pressure	Output pressure	Pressure ratio	Min. angle at switching off	Exergy efficiency
3 bar_{abs}	5-5.5 bar_{abs}	1.43-1.57	270°	23.0 %
4 bar_{abs}	6-6.5 bar_{abs}	1.5-1.625	240°	33.6 %
5 bar_{abs}	7-7.5 bar_{abs}	1.4-1.5	240°	36.9 %
5 bar_{abs}	7.5-8 bar_{abs}	1.5-1.6	240°	37.1 %

The overall efficiency of the smaller configuration is about 12 to 22 percentage points lower than the efficiency obtained with the larger configuration. This is mainly caused by the larger percentage of dead volume in comparison to the chamber volume. As the driving power of the smaller motor is lower, friction losses have a larger influence on the overall efficiency which is revealed in the efficiency decrease with lower supply pressure.

5 Summary and Conclusion

The paper shows a novel concept of pneumatic pressure boosters based on radial piston units. The motor is actuated by two fast switching valves per cylinder whereas the compressor is passively controlled by two check valves. To identify the efficiency potential of the concept, a simulation study was conducted. Afterwards, a working model was built and the exergy efficiency was measured.

The simulation results show exergy efficiency values up to 71 %. This large potential was verified in the experimental study where exergy efficiency values up to 59 % were identified. The measurements show an increase of efficiency with driving pressure as well as pressure ratio. It is shown that the larger configuration, comprising of a five cylinder motor and a three cylinder compressor, has significantly better efficiency than the smaller configuration comprising of two three cylinder units with different piston diameters.

A reduction of dead volumes leads to an increase in efficiency as the output mass flow is increased and the input mass flow is reduced. In the functional model, a design using off-the-shelf components was implemented. This approach leads to large dead volumes of up to 22 % of the smaller compressor's cylinder chamber volume. Due to this fact the efficiency of the small booster configuration is lower.

An additional approach to increasing the efficiency is the reduction of friction losses. The pressure ratio is determined by the ratio between the driving torque and the load torque which comprises of the compressor torque and the friction torque. The pistons of the functional model presented in the paper are sealed using o-rings due to the available installation space. In the future, a more sophisticated sealing concept shall be designed and implemented to reduce the necessary driving torque and therewith the input air mass.

6 Acknowledgements

The authors thank the Research Association for Fluid Power of the German Engineering Federation VDMA for its financial support. Special gratitude is expressed to the participating companies and their representatives in the accompanying industrial committee for their advisory and technical support.

Nomenclature

Variable	*Description*	*Unit*
$c_{\mathrm{p,air}}$	Specific, isobaric heat capacity of air	[J/kgK]
E_{air}	Exergy contained in the air mass	[J]
$F_{\mathrm{G}}, F_{\mathrm{TG}}$	Pressure force / Pressure force in tangential direction	[N]
$h_{\mathrm{amb}}, h_{\mathrm{air}}$	Specific enthalpy of air at ambient/current conditions	[J/kg]
IDC, ODC	Inner/outer dead center	[°]
$l_{\mathrm{crank}}, l_{\mathrm{rod}}$	Crank/rod length	[m]
M	Torque	[Nm]
m_{air}	Air mass	[kg]
n	Polytropic coefficient	[-]
n	Rotational speed	[1/s]
$p_{\mathrm{amb}}, p_{\mathrm{sup}}, p_{\mathrm{out}}$	Ambient/supply/output pressure	[bar]
R	Specific gas constant of air	[J/kgK]
s	Piston stroke	[m]
$s_{\mathrm{amb}}, s_{\mathrm{air}}$	Specific entropy of air at ambient/current conditions	[J/kgK]
$T_{\mathrm{amb}}, T_{\mathrm{sup}}, T_{\mathrm{out}}$	Ambient/supply/output temperature	[K]
V	Volume	[m³]
$W_{\mathrm{el,in}}$	Electrical energy supplied to the system	[J]
z_{cyl}	Number of cylinders	[-]
ζ	Exergy efficiency	[-]
λ_{s}	Push rod ratio	[-]
ρ	Density	[kg/m³]
φ	Rotational position	[°]

References

/1/ Achten, P., van den Brink, T., et al., A four-quadrant hydraulic transformer for hybrid vehicles. In: *The 11th Scandinavian International Conference on Fluid Power, SICFP'09*, 2009.

/2/ Dluzik, Klaus, Entwicklung und Untersuchung energiesparender Schaltungskonzepte für Zylinderantriebe am Drucknetz, Dissertation, Aachen, 1989.

/3/ Vukovic, M., Sgro, S., Murrenhoff, H., STEAM: A Mobile Hydraulic System With Engine Integration. In: *ASME/BATH 2013 Symposium on Fluid Power and Motion Control*, 2013.

/4/ Pischinger, S., Grundlagen der Verbrennungsmotoren Energiewandlungsmaschinen II (in German Language), 7th ed., Aachen, 2009.

/5/ Murrenhoff, H., Reinertz, O., Fundamentals of Fluid Power Part 2: Pneumatics, Shaker, Aachen 8, 2014.

/6/ Baehr, H., Kabelac, S., Thermodynamik (in German Language), Springer Berlin Heidelberg, Berlin, Heidelberg, 2012.

/7/ Krichel, S., Sawodny, O., Exergy Flow Diagrams as Novel Approach to Discuss the Efficiency of Compressed Air Systems. In: *8th International Fluid Power Conference (8th IFK)*, 2012.